L/F-CIPS: Collaborative indoor positioning for smartphones with lateration and fingerprinting

Pavel Pascacio, Joaquín Torres-Sospedra, Sven Casteleyn,
Elena Simona Lohan *Senior Member, IEEE*, Jari Nurmi *Senior Member, IEEE*

***Abstract*— The demand for indoor location-based services and the wide availability of mobile devices have triggered research into new positioning systems able to provide accurate indoor positions using smartphones. However, accurate solutions require a complex implementation and long-term maintenance of their infrastructure. Collaborative systems may help to alleviate these drawbacks. In this paper, we propose a smartphone-based collaborative architecture using neural networks and received signal strength, which exploits the built-in wireless communication technologies in smartphones and the collaboration between devices to improve traditional positioning systems without additional deployment. Experiments are carried out in two real-world scenarios, demonstrating that our proposed architecture enhances the position accuracy of traditional indoor positioning systems.**

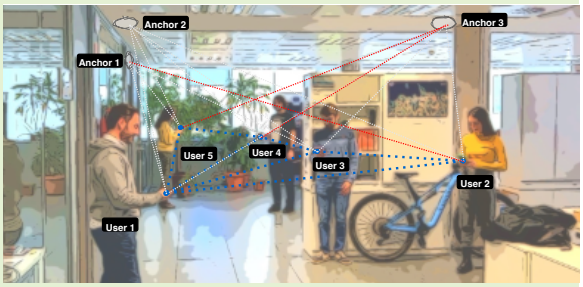

***Index Terms*— Collaborative Indoor Positioning, Fingerprinting, Lateration, Received Signal Strength, Neural Networks.**

I. Introduction

THE global indoor Location-Based services (LBS) is a rising market which will reach USD 35.69 billion by the end of 2026 [1]. Traditional Indoor Positioning Systems (IPSs) based on Bluetooth Low Energy (BLE) anchors and IEEE 802.11 Wireless LAN (Wi-Fi) Access Points (APs) are widely implemented in LBS applications [2]–[5]. The main benefits include the easy deployment of BLE anchors and wide availability of Wi-Fi [6], the ubiquity of both technologies in users' devices (e.g., smartphones and wearables) [7], and their compatibility with straightforward positioning approaches based on Received Signal Strength (RSS).

Manuscript received xx September 2022; revised xx September 2022; accepted xx xxxx 2022. Date of publication xx xxxx 2022; date of current version xx xxxx 2022. The authors gratefully acknowledge funding from European Union's Horizon 2020 RIA programme under the Marie Skłodowska Curie grant agreement No. 813278 (A-WEAR: A network for dynamic wearable applications with privacy constraints) and No. 101023072 (ORIENTATE: Low-cost Reliable Indoor Positioning in Smart Factories). The associate editor coordinating the review of this article and approving it for publication was Prof. Name Surname (Corresponding authors: J. Torres-Sospedra and S. Casteleyn).

Pavel Pascacio de los Santos with the Electrical Engineering Unit, Tampere University, 33720 Tampere, Finland, and Institute of New Imaging Technologies, Universitat Jaume I, 12071 Castellón de la Plana, Spain. (e-mail: pascacio@uji.es)

Sven Casteleyn is with the Institute of New Imaging Technologies, Universitat Jaume I, Castellón de la Plana 12003, Spain (e-mail: sven.casteleyn@uji.es).

Elena Simona Lohan and Jari Nurmi are with the Electrical Engineering Unit, Tampere University, 33720 Tampere, Finland.(e-mail: elena-simona.lohan@tuni.fi and jari.nurmi@tuni.fi)

Joaquín Torres-Sospedra is with the Centro ALGORITMI, Universidade do Minho, 4800-058 Guimarães, Portugal (e-mail: info@jtorr.es).

Digital Object Identifier 10.1109/JSEN.2023.XXXXXXXXX

BLE and Wi-Fi were designed to provide wireless communications [7], but have drawbacks when used for positioning. The non-linear RSS fluctuations [8], [9], heterogeneity of devices (hardware & software), user interaction (carry & hold patterns) [10], and inadequate distribution of anchors [11] are the main sources for accuracy degradation in RSS-based positioning. To mitigate them, advanced lateration and fingerprinting methods are applied to Wi-Fi and BLE RSS-based positioning [12]. However, the most accurate current solutions require complex implementation and long-term maintenance of their infrastructure [2], which increases the cost and makes them inaccessible for a wide range of applications.

In addition to the traditional IPSs, there exists a variant named Collaborative Indoor Positioning System (CIPS). A CIPS exploits the duality of wireless communication technologies (e.g., Wi-Fi and BLE) for use as positioning technologies and information exchange between users/devices to estimate their relative distance and position[12]. The main benefits of CIPS over the convectional IPS reported in the literature are: its relatively inexpensive and straightforward infrastructure implementation while improving the accuracy of the positioning of the system, thanks to the use of neighbouring devices as an extended infrastructure; it mitigates positioning inaccuracies due to inappropriate anchors distributions; and it reduces positioning errors due to Non-line-of-sight (NLOS) environments.

Despite the benefits of CIPSs to improve traditional IPS without additional deployment cost, a detailed comparison of those benefits over the two most popular IPSs (fingerprinting and lateration) based on BLE anchors and Wi-Fi AP using heterogeneous mobile devices has not yet been carried out.

In this paper, we focus on enhancing the positioning accuracy of traditional IPSs based on RSS lateration with BLE and RSS fingerprinting with BLE & Wi-Fi. We experimentally tested our proposed implementations in two real-world scenarios. The main contributions of this paper include:

- We propose two novel CIPS variants based on a straightforward L/F-CIPS (Lateration/Fingerprinting-CIPS) architecture that utilizes Multilayer Perceptron (MLP) Artificial Neural Networks (ANNs). The *Variant 1* is based on Received Signal Strength (RSS) lateration and the *Variant 2* is based on RSS fingerprinting.
- We comprehensively evaluate both variants under various conditions (i.e., diverse distribution of collaborative users/devices in the environment, different NLOS conditions) and indoor environments (office and lobby scenarios).
- We analyze the accuracy for different distances and distributions among smartphones.

II. Related work

Pascacio *et al.* [12] provides an exhaustive review of CIPSs analyzing their technologies, techniques and methods used. Accordingly, with the results reported, Wi-Fi and BLE coupled with lateration and fingerprinting methods are widely adopted for position estimation. Within the diverse research avenues to improve them, reaching a trade-off between positioning accuracy and deployment & maintenance cost of the systems is one of the most important topics.

In the context of lateration, Ozer and John [13] reduced the fluctuation of the RSS and improved the accuracy of BLE IPS using the Kalman filter. Similarly, Zafari *et al.* [14] introduced a method that sequentially combines Particle Filter (PF) and Extended Kalman Filter (EKF) to lessen the impact of multipath effects and noise on the RSS and improve accuracy up to $\approx 34\%$. Booranawong *et al.* [15] proposed a method based on zone area boundaries to determine if the estimated position needed to be compensated. The results showed that the proposed method improves the traditional lateration by $\approx 60\%$. Pascacio *et al.* [16] proposed a lateration method based on a combinatorial BLE anchor selection to enhance the positioning accuracy of lateration methods, with an error reduction of $\approx 14\%$ with respect to the traditional lateration in an office scenario.

In the case of fingerprinting, crowdsourcing is very popular. Santos *et al.* [17] proposed a method for creating indoor maps and fingerprints automatically that only uses unannotated crowdsourced data from smartphones, using sensors such as accelerometer, gyroscope, magnetometer, and Wi-Fi. The experimental results showed that the proposed approach presented similar floor plans and fingerprints to those acquired manually. Likewise, Li *et al.* [18] presented a smartphone crowdsourcing to create an indoor Wi-Fi radio map based on geomagnetic and inertial data. The computation of magnetic similarity, the grouping of road segments, and the creation of route maps all demonstrate the method's effectiveness, nevertheless, the approach is only applicable in indoor environments with obvious straight corridors.

Considering smartphone-based IPSs, the new trends explore the collaboration among users. Taniuchi *et al.* [19] proposed a CIPS based on a spring model and homogeneous smartphones using Wi-Fi-fingerprinting and BLE RSS. The optimized spring model was used to correct the positioning errors estimated by fingerprinting, providing an improvement of accuracy within 2.7%-32.6% in several scenarios. Pascacio *et al.* [11] proposed a CIPS to improve positioning accuracy of BLE lateration using ANN. The results of the experiments performed in an office environment with heterogenous devices demonstrated that the CIPS proposed decreased $\approx 13\%$ the mean positioning error with respect to the lateration baseline.

Contrary to the previously presented works, we propose two CIPS variants, based on a modular and straightforward L/F-CIPS architecture that uses MLP ANNs and heterogeneous mobile devices, for improving the positioning accuracy of IPSs considering two diverse technologies (BLE and Wi-Fi) and methods (lateration and fingerprinting). Also, we experimentally test them in two real-world scenarios considering the effect of distance distribution between devices on the accuracy.

III. Collaborative system overview

The structure of our two variants of L/F-CIPS relies on an architecture, which considers the findings and recommendations presented in our CIPS systematic review [12].

In our architecture, we consider a modular decentralized architecture. A modular design allows us to divide the system into independent parts that can be evaluated, configured, improved, and re-used. Unlike the breakdown of the CIPSs introduced in our systematic review, which divided the CIPSs into two phases (non-collaborative and collaborative), we designed our architecture considering three phases. We have included an additional phase that deals with device heterogeneity. Specifically, the new phase performs the calibration and registration of the collaborative devices.

We consider a decentralized architecture for our L/F-CIPS scheme, given the benefits identified in our systematic review. Under the decentralized architecture, each device can execute the algorithms and exchange information with the neighboring devices without using a central node. In addition, the selected architecture enables the devices to be independent. Devices can execute a positioning algorithm or use a technology different from the rest. For example, some devices can use BLE lateration, while the rest can use Wi-Fi fingerprinting.

The infrastructure needed for our L/F-CIPS architecture depends on the technology implemented in the non-collaborative phase. The non-collaborative phase can be used as infrastructure-based (e.g., using BLE beacons deployed in the environment for positioning purposes) or signals of opportunity with no additional infrastructure (e.g., using Wi-Fi APs present in the environment). In contrast, the proposed collaborative phase is infrastructure-less, as it uses embedded wireless technologies in the mobile devices.

The main objectives of our proposed L/F-CIPS architecture are:

- To provide a mobile device-based L/F-CIPS architecture using MLP ANNs to enhance the performance (e.g., position accuracy, complexity, etc.) of traditional IPSs.

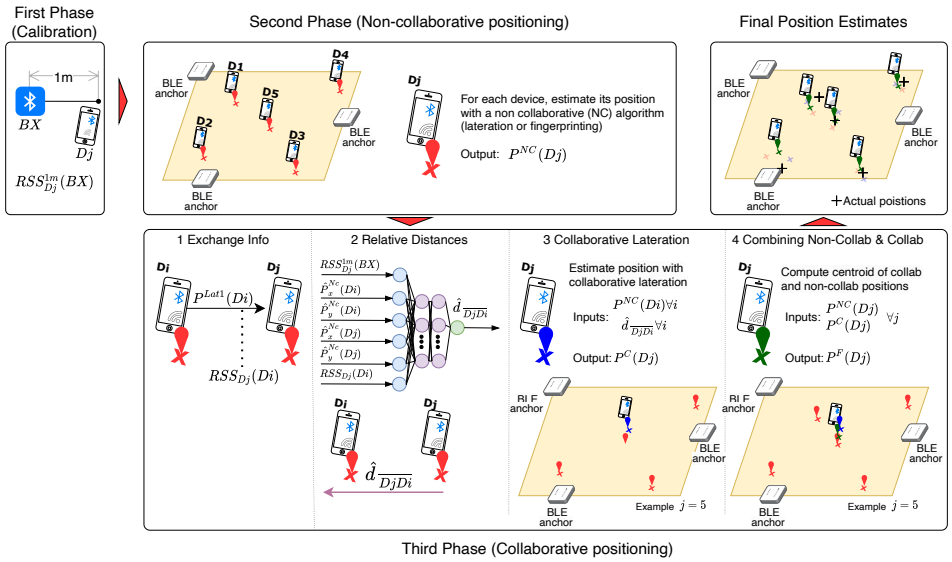

Fig. 1. L/F-CIPS architecture. Example of position estimation of a target device (D5) using neighboring devices (D1-D4)

- To propose a versatile and straightforward L/F-CIPS architecture that allows us to develop and evaluate the performance of diverse collaborative indoor positioning technologies, techniques, and methods.

Fig. 1 presents our proposed L/F-CIPS architecture through an example, which improves the position of device 5 using the neighboring devices. The first phase calibrates and registers devices, the second estimates device positions non-collaboratively, and the third phase collaboratively refines the estimated position of the target device/user (i.e., device 5). An iterative refinement of the position estimates would be possible at the expense of a higher computational cost, limiting real-time operation. Thus, we focus in this paper on the single iteration approach.

Our proposed L/F-CIPS architecture is used to implement two variants. *Variant 1* is based on BLE lateration and *Variant 2* on BLE and Wi-Fi fingerprinting. Details of the architecture's phases are described in the following subsections.

A. First phase: configuration phase

The first phase, which is identically for both L/F-CIPS variants, is dedicated to the calibration and registration of mobile devices. It identifies mobile devices and stores the required parameters to be processed in the collaborative algorithm. The procedure is requesting each new user to stand at a floor mark, $1\,\mathrm{m}$ away from a reference anchor (BX) during $60\,\mathrm{s}$, in order to measure and record some RSS values (i.e., $RSS^{1m}_{RX}(BX)$) and then average them to get only one value per device. The reference anchor broadcasts BLE advertisements and can be installed, for example, at the main entrance of the scenario. For each (new) device, this quick calibration process is only carried out once. A practical implementation of this procedure could be to connect the calibration with the electronic door-locking system installed in mobile devices.

B. Second phase: non-collaborative phase

The second phase corresponds to the non-collaborative part, which is used to determine the initial position of each device. In the non-collaborative phase, the mobile devices act as receivers (RX), while a custom infrastructure based on Wi-Fi APs or BLE anchors acts as emitters (TX). We implemented a different stand-alone positioning method for each variant.

Variant 1 is based on lateration and BLE technology (stand-alone BLE-RSS lateration method) and *Variant 2* is based on fingerprinting-k-Nearest Neighbors (k-NN) and Wi-Fi and BLE technologies (stand-alone BLE/Wi-Fi-RSS fingerprinting-k-NN method).

1) Stand-alone BLE-RSS lateration method: The lateration method used to estimate the position relies on the Logarithm Distance Path Loss (LDPL) model, a minimization problem, and the Levenberg-Marquardt algorithm for weighted non-linear least-squares to solve the minimization problem. The LDPL model (see Eq. (1)) correlates the attenuation of the signal strength as it propagates through space and the distance between the transmitter and the receiver:

$$RSS^{d}_{RX}(TX) = RSS^{1m}_{RX}(BX) - 10\,\eta\,log\left(\frac{d}{d_0}\right) \qquad (1)$$

where $RSS^{d}_{RX}(TX)$ denotes the RSS value measured by the receiver (RX), which is at a distance d from the transmitter (TX); $RSS^{1m}_{RX}(BX)$ denotes the RSS value measured by the receiver (RX), which is at a distance of $1\,\mathrm{m}$ from the BLE anchor transmitter (BX); The transmitter could be a BLE anchor or a mobile device; and η is the path-loss attenuation factor.

The stand-alone lateration approach is described by the Algorithm 1, and its working procedure is outlined as follows:

- **1st step:** Gather the RSS from BLE anchors $(RSS^{d}_{RX}(TX))$ that are reachable in a time window (tw) of $60\,\mathrm{s}$, excluding those that are not part of the deployment scenario (input data for Algorithm 1);

- **2nd step:** Group the RSS gathered in **1st step** by anchors, then remove the outliers of each group, which are those values outside of 25 and 75 percentiles (lines 1–2 in Algorithm 1);
- **3rd step:** Average RSS value per anchor by applying the average operator to the RSS values in each group. (line 3 in Algorithm 1);
- **4rd step:** Choose those BLE anchors whose averaged RSS value is equal to or within a pre-set threshold (lines 4–8 in Algorithm 1);
- **5th step:** Estimate the relative distance between the chosen BLE anchors in **4rd step** and the target position of the device/user by applying the LDPL model (eq.(1)) (line 9 in Algorithm 1);
- **6th step:** Estimate the position of the device/user $\hat{\mathbf{P}}^{Lat1}$ by applying the Levenberg-Marquardt Weighted Least Squares (L-MWLS) lateration, which uses the data computed in the **5th step**, the weights, and the Ground-Truth (GT) of the BLE anchors. The weight for every BLE anchor is calculated as the inverse of the estimated distance between the anchor and the device. $Lat1$ refers to L-MWLS lateration in the stand-alone phase.

The $threshold$ and the attenuation factor (η) values are $-83\,\mathrm{dBm}$ and 2.1 respectively, as we used before in [16] and which are aligned with values proposed in the literature [20]. The devices used in the collaborative positioning approach have their own $RSS^{1m}_{RX}(BX)$ value according to the data gathered during the device calibration phase (see Table I).

TABLE I
$\boldsymbol{RSS^{1m}_{RX}(BX)}$ PER DEVICE IN BOTH SCENARIOS

ID/RX	Device name	Model	$RSS^{1m}_{RX}(BX)$ (dBm)	Scenario
1	Galaxy S8	SM-G950F	-68.88	Both
2	Lenovo Yoga Book	YB1-X90F	-74.75	Office
3	Galaxy A7 Duos	SM-A7100	-62.39	Office
4	Galaxy S6	SM-G920F	-62.99	Office
5	Honor 20 Lite	HRY-LX1T	-62.11	Lobby
6	Galaxy A5	SM-A500FU	-78.79	Office
7	Galaxy S6 Edge	SM-G928F	-61.17	Lobby
8	Huawei P40 Lite	CDY-NX9A	-69.74	Lobby
9	Galaxy A12	SM-A125F	-66.79	Lobby

2) Stand-alone Wi-Fi/BLE-RSS fingerprinting-k-NN method:

Our stand-alone fingerprinting-k-NN method is described by the Algorithm 2 and based on the k-NN algorithm used in [6]. Its workflow is as follows:

- **1st step:** Gather the RSS from BLE anchors/Wi-Fi APs ($RSSI_{RX}(TX)$) during a time window (tw) of $10\,\mathrm{s}$, excluding those that do not are part of the fingerprinting radio map (input data for Algorithm 2);
- **2nd step:** Group the RSS, gathering in **1st step**, by BLE anchor/Wi-Fi AP, (line 1 in Algorithm 2);
- **3rd step:** Average the RSS value per BLE anchor/Wi-Fi AP by applying the average operator to the RSS values in each group. (line 2 in Algorithm 2);
- **4th step:** Estimate the position of the device/user ($\hat{\mathbf{P}}^{FP}(RX) = [\hat{P}^{FP}_x(RX), \hat{P}^{FP}_y(RX)]$) using the $FPradiomap$, the RSS values processed in the **3rd** step, and the k-NN algortihm. (line 3 in Algorithm 2);

Algorithm 1 Stand-alone lateration

Input: Deployed anchors information collected within a time window tw: $RSS^{d}_{RX}(TX)$ values and GT
Input: LDPL: $\eta = 2.1$ and $RSS^{1m}_{RX}(BX)$
Input: $threshold$
Output: Estimated device/user position $\hat{\mathbf{P}}^{Lat1}(RX)$
1: Group the $RSS^{d}_{RX}(TX)$ values by beacon
2: Remove $RSS^{d}_{RX}(TX)$ outliers values of each group
3: Average $RSS^{d}_{RX}(TX)$ values of each group : $\overline{RSS^{d}_{RX}(TX)}$
4: **for** $i \leftarrow 1$ **to** number of $\overline{RSS^{d}_{RX}(TX)}(i)$ **do**
5: **if** $(\overline{RSS^{d}_{RX}(TX)}(i) \geq threshold)$ **then**
6: Include i-th anchors to reference anchors set $(ref_{anchorset})$
7: **end if**
8: **end for**
9: Estimate the distances between anchors of $ref_{anchorset}$ and the device/user position using Eq.1
10: Estimate the device/user position ($\hat{\mathbf{P}}^{Lat1}(RX) = [\hat{P}^{Lat1}_x(RX), \hat{P}^{Lat1}_y(RX)]$) using the Levenberg-Marquardt Weighted Least Squares method

The fingerprint radio map ($FPradiomap$), used as input, contains the information of the RSS values and the (x,y) coordinates where they were gathered. In the k-NN algorithm, we considered $k = 5$, which was chosen experimentally to give the model's ability to generalize to new data.

Algorithm 2 Stand-alone fingerprinting-KNN

Input: Information collected, within a time window tw, from the BLE anchors/Wi-Fi APs available: $RSS_{RX}(TX)$ values
Input: k value
Input: $FPradiomap$ with location labels
Output: Estimated device/user position $\hat{\mathbf{P}}^{FP}(RX)$
1: Group the $RSS_{RX}(TX)$ values by BLE anchor/Wi-Fi AP
2: Average $RSS_{RX}(TX)$ values of each group : $\overline{RSS_{RX}(TX)}$
3: Estimate the device/user position ($\hat{\mathbf{P}}^{FP}(RX) = [\hat{P}^{FP}_x(RX), \hat{P}^{FP}_y(RX)]$).

C. Third phase: collaborative phase

The third phase is the collaborative phase. In this phase, we estimate the position of the device/user based on the collaboration of the surrounding devices/users. In the collaborative phase, we have just a set of mobile devices which act as receivers and emitters. When computing the position for a particular target device (TD) in a collaborative way, the remaining devices act as neighborhood devices (NDs). The final position is estimated in 4 stages: 1) the devices exchange their information via wireless communication (i.e., BLE advertisement); 2) we estimate the relative distance between them based on RSS values and a MLP ANNs model; 3) we apply a collaborative lateration algorithm to estimate the device/user' position, and 4) we apply an algorithm to combine the estimated position of the non-collaborative and collaborative phases. Stages 1, 3, and 4 are the same for both implemented L/F-CIPS variants. However, the MLP ANNs

architecture implemented in stage 3 is different for each of them. Extended description includes:

1) Information exchanged between devices/users: Fig. 1 (third phase–part 1) shows the process through which the devices sense the environment to gather and share the information required to compute collaboratively their own position.

Each device shares its estimated position (i.e., using ibeacon protocol), and measures the RSS values of neighbor devices within a time window (wt) of $60\,\mathrm{s}$ and $10\,\mathrm{s}$ for first and second CIPS variant, respectively. In detail, the information collected are: 1) the received RSS from the neighbor device ($RSSI_{RX}(TX)$), 2) the estimated position of the neighbor ($[\hat{P}_x^{Nc}(TX), \hat{P}_y^{Nc}(TX)]$), 3) the estimated position of the target device ($[\hat{P}_x^{Nc}(RX), \hat{P}_y^{Nc}(RX)]$), and 4) the calibration RSS of the target device ($RSS_{RX}^{1m}(BX)$).

2) Estimation of the relative distance between devices: We estimate the relative distance between devices using a MLP ANNs model. The input of the MLP neural network model corresponds to the information exchanged between each pair (target device–neighbor device) described in Section III-C.1, and the output to the estimated distance of that specified pair.

The first architecture is designed for *Variant 1* of the L/F-CIPS, which uses only BLE technology and lateration method to estimate position in the office scenario. The architecture is composed of one input layer with six neurons, one hidden layer with three neurons, and one output layer as shown in Fig. 2. The activation and training functions used are the hyperbolic tangent, and the scaled conjugate gradient backpropagation, respectively, and 50 epochs were used.

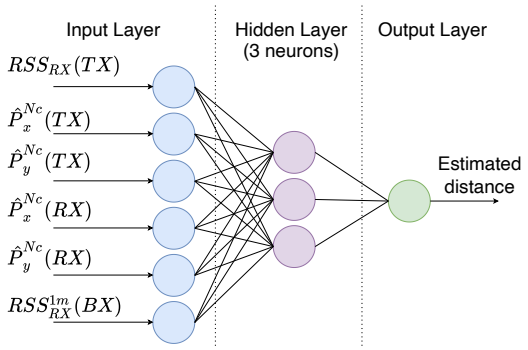

Fig. 2. MLP neural network model architecture for *Variant 1* of the L/F-CIPS. Used to estimate the relative pairwise distance between the target and neighboring devices/users.

The second architecture, corresponding to *Variant 2*, allows us to cope with diverse scenarios (i.e., office and lobby), and fingerprint-based positioning with BLE and Wi-Fi). In detail, the second architecture consists of one input layer, three hidden layers, and one output layer as shown in Fig. 3. The first hidden layer has three neurons and the second and third layers have fourteen neurons each. We used the hyperbolic tangent sigmoid (tangsig) activation function, the conjugate gradient backpropagation (trainscg) training function, and 12 epochs.

Fig. 1 (third phase–part 2) shows the collaborative scenario after estimating the relative distance between devices. In the scenario, the distances estimated by the MLP ANNs model are

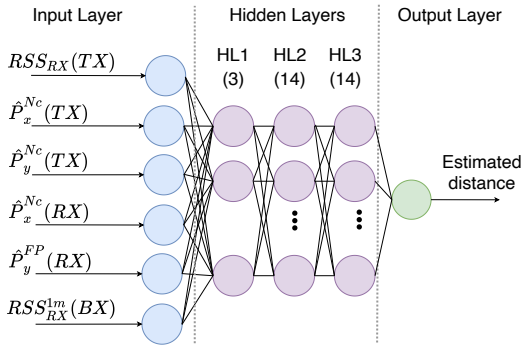

Fig. 3. MLP neural network model architecture for *Variant 2* of the L/F-CIPS. Used to estimate the relative pairwise distance between the target and neighboring devices/users.

depicted by the purple lines. The two selected models were selected after MLP tuning described in Section IV-B.

3) Collaborative lateration algorithm: The collaborative lateration algorithm implemented is similar to the one proposed in Section III-B.1 and described by the Algorithm 1. The main differences are with the data for lateration.

First, the anchors used by the collaborative lateration are the neighbouring devices/users, whose position is estimated by the stand-alone lateration (*Variant 1* of the L/F-CIPS) or fingerprinting (*Variant 2* of the L/F-CIPS), instead of the BLE anchors deployed in the scenario with a well-known position. Second, rather than using the LDPL model to estimate the relative distance between neighboring devices/users and the target device/user, we use a MLP neural network model. The input data needed in the collaborative lateration algorithm are the initial position non-collaboratively estimated of surrounding devices and the relative distance between the target and surrounding devices estimated by the MLP ANNs.

Fig. 1 (third phase–part 3) depicts the inputs and output obtained after performing the collaborative lateration algorithm. Also, the two kinds of estimated positions are depicted by the orange (non-collaboratively estimated position) and blue (collaborative estimated position) pushpins, which are the inputs for the midpoint line algorithm (see Section III-C.4).

4) Combining stand-alone and collaborative estimated positions: The final estimated position is the centroid of the non-collaboratively estimated position and the collaboratively one (see Eq. (2) and Eq. (3)):

$$\hat{P}_x^F(RX) = \frac{\hat{P}_x^{Nc}(RX) + \hat{P}_x^C(RX)}{2} \tag{2}$$

$$\hat{P}_y^F(RX) = \frac{\hat{P}_y^{Nc}(RX) + \hat{P}_y^C(RX)}{2} \tag{3}$$

Where $\hat{\mathbf{P}}^F(RX) = [\hat{P}_x^F(RX),\ \hat{P}_y^F(RX)]$ denotes the final estimated position of device/user RX, with $RX = \{1, 2....N\}$ and N the number of devices. $\hat{P}_x^{Nc}(RX)$ and $\hat{P}_y^{Nc}(RX)$ denotes the position non-collaboratively estimated with the stand-alone lateration or fingerprinting depending on whether it is implemented, *Variant 1* or *Variant 2* of the L/F-CIPS. $\hat{P}_x^C(RX)$ and $\hat{P}_y^C(RX)$ denotes the position collaboratively estimated with the collaborative lateration ($\hat{P}_x^{lat_2}(RX)$ and $\hat{P}_y^{lat_2}(RX)$), both for device/user RX.

Fig. 1 (third phase–part 4) depicts the inputs and output obtained after performing the midpoint line algorithm. Also, it shows the final collaborative scenario, with the three positions (non-collaboratively, collaboratively and final) computed for each device as orange, blue and green pushpins, respectively. As can be observed, the positioning error between the devices' current (red crosses) and final estimated position (green pushpin) was reduced in most cases.

5) Full collaborative workflow: The pseudo-code for the proposed L/F-CIPS is in Algorithm 3 and outlined as follows:

- **1st step:** Group the RSS readings by device, then remove of each group the outliers, values outside of 25 and 75 percentiles (lines 1–2 in Algorithm 3);
- **2rd step:** Average the RSS values per each device/user, getting one averaged RSS value per device/user (line 3 in Algorithm 3);
- **3th step:** Estimate the relative distances between the neighboring devices/users and the target device/user, by applying the MLP ANNs model. The inputs of MLP ANNs model are: $RSSI_{RX}(TX)$, $RSSI_{RX}^{1m}(BX)$, ($\hat{P}_x^{Nc}(TX)$,$\hat{P}_y^{Nc}(TX)$,$\hat{P}_x^{Nc}(RX)$,$\hat{P}_y^{Nc}(RX)$), and (input values in Algorithm 3);
- **4th step:** Estimate collaboratively the position of the device/user ($\hat{\mathbf{P}}^{C}(RX)$) by applying the Levenberg-Marquardt Weighted Least Squares (L-MWLS) lateration method, which input data are the relative distances estimated by the MLP ANNs model (**3th step**), the weights, and the estimated position ($\hat{\mathbf{P}}^{Nc}(TX)$) of each neighboring device/user. The weight value for every anchor is calculated as the inverse of its distance square with respect to the device/user;
- **5th step:** Compute the final estimated position of the device/user ($\hat{\hat{\mathbf{P}}}^{F}(RX)$) using the formula expressed in Eq. (2) and Eq. (3), considering the position collaborative and non-collaboratively estimated, $\hat{\mathbf{P}}^{Nc}(RX)$ and $\hat{\mathbf{P}}^{C}(RX)$, respectively. (RX) is the identifier of the device/user to estimate its position.

Algorithm 3 Collaborative module

Input: Collaborative devices information collected within a time window tw: $RSS_{RX}(TX)$, $RSS_{RX}^{1m}(BX)$, and ($\hat{P}_x^{Nc}(TX)$,$\hat{P}_y^{Nc}(TX)$,$\hat{P}_x^{Nc}(RX)$,$\hat{P}_y^{Nc}(RX)$)

Output: Improved estimated device/user position ($\hat{\hat{\mathbf{P}}}_{dev}^{F}(n)$)

1: Group the $RSS_{RX}(TX)$ values by device
2: Remove $RSS_{RX}(TX)$ outliers values of each group
3: Average $RSS_{RX}(TX)$ values of each group: $\overline{RSS_{dev}}(i)$
4: Estimate the relative distance between the target device and the near collaborative devices using the trained ANN model
5: Estimate the device/user's position ($\hat{\mathbf{P}}^{C}(RX)$) using the Levenberg-Marquardt Weighted Least Squares (L-MWLS) lateration method
6: Compute the final estimated device/user's position ($\hat{\hat{\mathbf{P}}}^{F}(RX)$) using the midpoint line algorithm of in Eq. (2) and Eq. (3)

It should be noted that the stand-alone method used to estimate non-collaboratively the user/device position as well as the MLP ANNs model selected and its inputs depend on the L/F-CIPS variant implemented.

IV. Experimental Setup

This section presents the experimental setup in order to: 1) assess the feasibility and advantages of our proposed L/F-CIPS architecture; 2) evaluate the proposed ANN-based estimator of relative distances under different indoor scenarios and technologies and 3) study how relative distances and NLOS conditions among devices impact the L/F-CIPS positioning error.

A. Scenarios and hardware

We selected two real-world scenarios, office, and lobby scenarios, to perform the data collection and experimentally test the IPS and *Variant 1* (only office scenario) and *Variant 2* (both scenarios) of the L/F-CIPS proposed. The office scenario, located at Universitat Jaume I, Spain, covers an approximate area of 16.7×10.8 m^2 and includes furniture such as chairs, desks, desktop computers, bookshelves, and concrete metal-reinforced pillars, as is sketched in Fig. 4.

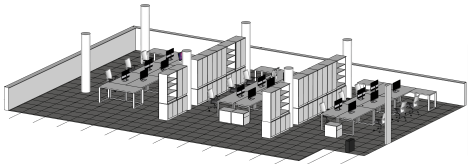

Fig. 4. 3D office scenario representation

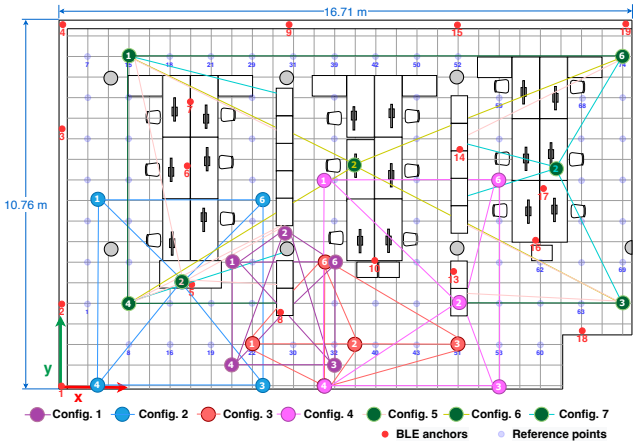

Fig. 5. Distribution of the configurations in the office scenario

The lobby scenario, located at Tampere University, Finland, covers an approximate area of 26.2×13.7 m^2 and includes furniture such as tables, seater sofas, lecture desks, office pod, and concrete metal-reinforced pillars, as is sketched in Fig. 6. Both scenarios provide rich and diverse NLOS conditions in the environment due to their particular geometry and furniture.

In the office and lobby scenarios, we designed collaborative configurations made up of 5 mobile devices. Each configuration presents a diverse distribution of mobile devices in the scenario, which provides different distances between devices and NLOS conditions. Fig. 5 presents the distribution of mobile devices in the office scenario and Fig. 7 the distribution of mobile devices in the lobby scenario for each configuration.

TABLE II
DEVICES' GROUND TRUTH BY CONFIGURATION IN OFFICE AND LOBBY SCENARIOS

ID/RX	Config. 1		Config. 2		Config. 3		Config. 4		Config. 5		Config. 6		Config. 7		Scenario
	x	y	x	y	x	y	x	y	x	y	x	y	x	y	
1	5.05	3.7	1.33	6.1	6.93	1.3	7.75	6.1	2.05	9.7	2.05	9.7	2.05	9.7	Office
2	6.55	4.55	4.49	3.05	9.93	1.3	11.75	2.75	3.6	3.3	8.7	6.4	14.66	6.45	Office
3	8.05	0.7	7.66	0.1	12.93	1.3	12.75	0.1	16.45	2.5	16.45	2.5	16.45	2.5	Office
4	5.05	0.7	1.33	0.1	9.03	0.1	7.75	0.1	2.05	2.5	2.05	2.5	2.05	2.5	Office
6	8.05	3.7	7.66	6.1	9.03	3.7	12.75	6.1	16.45	9.7	16.45	9.7	16.4	9.7	Office
1	2	3	0	0.5	9	2	6	0.5	0	0.5	0	0.5	—	—	Lobby
5	2	6	0	6	11	4.5	6	5.5	0	6	0	6	—	—	Lobby
7	5	3	14	6	15	2	12	5.5	14	6	14	6	—	—	Lobby
8	5	6	14	0.5	11	1	12	0.5	14	0.5	14	0.5	—	—	Lobby
9	1	4.5	12	3	12	2	9.5	4.5	1.5	2	7	3	—	—	Lobby

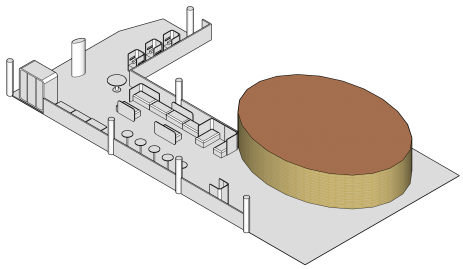

Fig. 6. 3D lobby scenario representation

Table II summarizes the GT coordinates of mobile devices by configuration in each scenario.

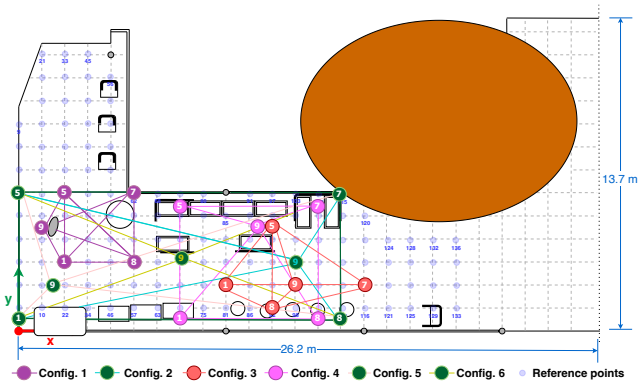

Fig. 7. Distribution of the configurations in the lobby scenario

Regarding the hardware, we used 9 diverse smartphones to perform the experiments in the scenarios. All of them were able to measure Wi-Fi and BLE RSS and transmit BLE packets using the iBeacon protocol. Details about devices were provided in Table I. In the office scenario, we deployed BLE anchors, which transmit at a power of $-4\,\mathrm{dBm}$ and a period of $250\,\mathrm{ms}$. Fig. 5 shows the distribution of BLE anchors (red points) and the reference points (blue points) used to build the BLE fingerprint radio map. In total, the BLE radio map contains 792 samples (72 ref. points $\times$ 11 samples). In the lobby scenario, we used the 67 already available Wi-Fi APs to build a Wi-Fi radio map. Fig. 7 shows the distribution of the 136 reference points (light blue points) used to build the Wi-Fi fingerprint radio map. In total, the Wi-Fi radio map contains 1088 samples (136 ref. points $\times$ 8 samples).

In *Variant 1* of the L/F-CIPS, we used 6 collaborative configurations (1 to 6), of the office scenario, made up of five mobile devices (1, 2, 3, 4, and 6), and the deployed BLE anchors (1, 4, 6, 9, 10, 17 and 19). We divided the data acquired, in the 6 configurations, into two datasets, ensuring that both datasets cover different zones of the scenario and the distances between devices and between anchors vary. Configurations 1, 4, and 5 are used for testing the model, and configurations 2, 3, and 6 are used for training & evaluation. The second dataset (training & evaluation) was randomly divided into training (70%) and validation (30%) to tune the MLP neural network. The testing dataset was used to test the MLP ANNs for relative distances, the stand-alone BLE-RSS lateration and the first CIPS variant.

In *Variant 2* of the L/F-CIPS, we used 6 collaborative configurations in the office (1-5, and 7) and lobby scenarios (1-6), made up of five smartphones, 1, 2, 3, 4, and 6 for the office and 1, 5, 7, 8, and 9 for the lobby scenario for the experimental test. In both scenarios, configurations 1, 4, and 5 are used for testing and configurations 3, 6, and 7 and configurations 2, 3 and 6 are used for training & evaluation in the office and lobby scenarios, respectively. In the same way as in *Variant 1*, the second dataset (training & evaluation) was randomly divided into training (70%) and validation (30%) to evaluate the MLP ANNs and the testing data set to test the stand-alone fingerprinting and *Variant 2*.

In both L/F-CIPS variants, data collection was carried out for 2 hours in each scenario. Also, simultaneously, the data from the deployed BLE anchors in the office scenario and Wi-Fi APs available in the lobby scenario were recorded.

B. Tuning the MLP neural network

In order to define the most suitable MLP architecture and its hyperparameters for our proposed L/F-CIPS model, we evaluate four architectures for the two implemented L/F-CIPS variants. The hyperparameters considered were the number of hidden layers, the number of hidden neurons and the activation function used –log-sigmoid (logsig) or hyperbolic tangent sigmoid (tansig)–.

1) MLP neural network for the Variant 1: For the *Variant 1*, we have considered 2 architectures with 1 hidden layer as a starting point, since it can model a wide number of nonlinear problems, and is useful for defining the activation function. In

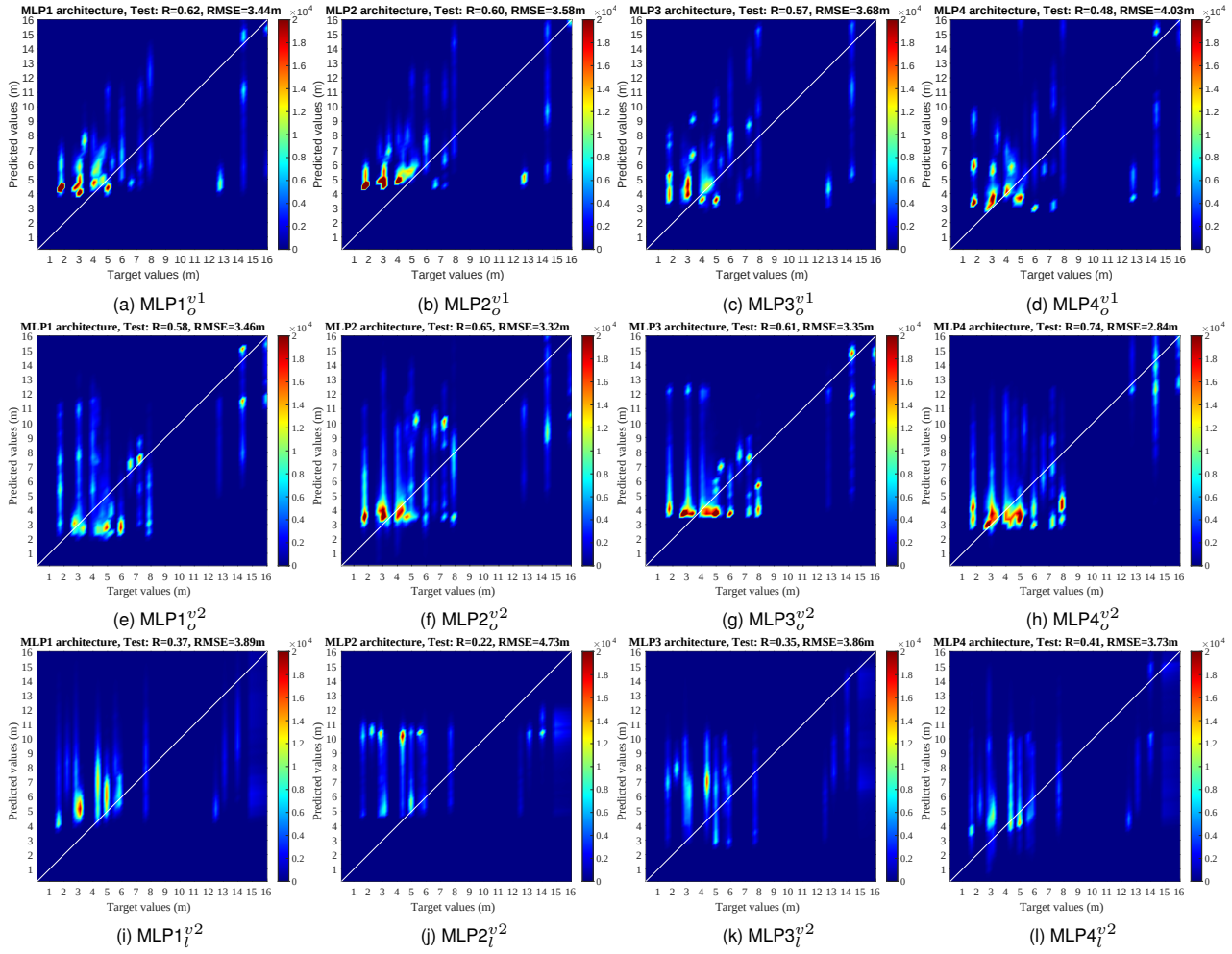

(a) MLP1$_o^{v1}$ (b) MLP2$_o^{v1}$ (c) MLP3$_o^{v1}$ (d) MLP4$_o^{v1}$

(e) MLP1$_o^{v2}$ (f) MLP2$_o^{v2}$ (g) MLP3$_o^{v2}$ (h) MLP4$_o^{v2}$

(i) MLP1$_l^{v2}$ (j) MLP2$_l^{v2}$ (k) MLP3$_l^{v2}$ (l) MLP4$_l^{v2}$

Fig. 8. Target vs predicted distances of the MLP neural network architectures

addition, we have considered 2 additional architectures with an extra layer. The hyperparameters are detailed in Table III.

TABLE III
TESTED MLP SET-UPS FOR THE *Variant 1* OF THE L/F-CIPS

Parameters	MLP1$_o^{v1}$	MLP2$_o^{v1}$	MLP3$_o^{v1}$	MLP4$_o^{v1}$
No. Hidden layers (HLs)	1	1	2	2
No. Neurons HL1	3	3	6	12
No. Neurons HL2	—	—	3	6
Training function	trainscg			
Activation function	tansig	logsic	tansig	tansig
Performance function	Mean Square error			

The results of comparing the real distance with the estimated distance in each of the 4 MLP ANN architectures are shown in Fig. 8 **(a-d)** as density scatter plots, as well as their correlation coefficient (R) and the Root Mean Square Error (RMSE). The scatter plots visualizes the relationship between target values (X-axis), predicted values (Y-axis), and the number of samples corresponding to each combination using a colour scale.

Based on the information presented in Fig. 8 **(a-d)**, we can observe that one hidden layer MLP architectures (MLP1$_o^{v1}$ and MLP2$_o^{v1}$) have lower RMSE than the two hidden layer ones (MLP3$_o^{v1}$ and MLP4$_o^{v1}$), and a greater correlation coefficient, namely 0.62 and 0.60 for MLP1$_o^{v1}$ and MLP2$_o^{v1}$, respectively. Specifically, comparing MLP1$_o^{v1}$ and MLP2$_o^{v1}$ through the density scatter plots, we notice that MLP1$_o^{v1}$ has a higher density of predicted values near to the real values (white diagonal line) than MLP2$_o^{v1}$.

Consequently, in terms of accuracy, one hidden layer MLP architectures are better able to estimate the distance. In particular, MLP1$_o^{v1}$, which uses a hyperbolic tangent sigmoid activation function (tansig) provides the best performance.

2) MLP neural network for the Variant 2: For the *Variant 2*, we have considered the best architecture for the first CIPS variant. As fingerprinting is less accurate than lateration, we considered more complex architectures, one with 2 hidden layers and two with 3 hidden layers. The hyperparameters for each architecture are detailed in Table IV.

TABLE IV
TESTED MLP SET-UPS FOR THE *Variant 2* OF THE L/F-CIPS

Parameters	MLP1$_{o\&l}^{v2}$	MLP2$_{o\&l}^{v2}$	MLP3$_{o\&l}^{v2}$	MLP4$_{o\&l}^{v2}$
No. Hidden layers (HLs)	1	2	3	3
No. Neurons HL1	3	3	3	3
No. Neurons HL2	—	6	6	14
No. Neurons HL3	—	—	6	14
Training function	trainscg			
Activation function	tansig			
Performance function	Mean Square error			

Similarly, the results of comparing the actual distance with the estimated distance in each of the 4 MLP neural network architectures are presented in Fig. 8 **(e-h)** and Fig. 8 **(i-l)** through density scatter plots, their correlation coefficient (R), and the RMSE for the office and lobby scenarios, respectively.

Based on Fig. 8 **(e-h)** for the office scenario with fingerprinting, we can observe that three hidden layer MLP architectures (MLP3_o^{v2} and MLP4_o^{v2}) have lower RMSE than the one hidden layer one (MLP1_o^{v2}), and a greater correlation coefficient, namely 0.61 and 0.74 for MLP3_o^{v2} and MLP4_o^{v2}, respectively. The architecture with two hidden layers, MLP2_o^{v2}, performs slightly better than MLP3_o^{v2} but worse than MLP4_o^{v2}. In terms of relative distances estimation, MLP4_o^{v2} is the best. Comparing the density scatter plots of MLP3_o^{v2} and MLP4_o^{v2}, we notice that the MLP architecture with a higher number of neurons in the second and third layers (MLP4_o^{v2}) has a higher density of predicted values near to the real values (white diagonal line) than the one with the lower number of neurons in the second and third layers (MLP3_o^{v2}).

Based on Fig. 8 **(i-l)** for the lobby scenario, we can observe a similar behaviour as in the office scenario with fingerprinting, but with minor differences arise as the worse reconstruction is provided with the two layer architecture, low density of predicted values near to the real values in the plot of MLP2_l^{v2}, in this case. In terms of accuracy, the architecture MLP4_l^{v2} is also the best to estimate relative distances in the lobby.

V. Results and Discussion

The main results of the evaluation of our two proposed L/F-CIPS variants are presented in this section. We have considered the RMSE, mean, median, 75$^{\text{th}}$, and 90$^{\text{th}}$ percentile as main evaluation metrics. In each scenario, we distributed the smartphones considering three distances among them, configuration 1 (short distances), configuration 4 (medium distances), and configuration 5 (large distances). Specifically, we present independently the results of each configuration used for testing to show the effect of the relative distance between collaborative devices and NLOS conditions on positioning accuracy in CIPS.

A. Results of Variant 1

Fig. 9 shows the Empirical Cumulative Distribution Function (ECDF) plots of each configuration set in the office scenario. The red lines represent the result for the first L/F-CIPS variant using MLP ANNs (collaborative approach) and the black lines for the stand-alone BLE-lateration (lateration baseline). In detail, Fig. 9 **(a)** presents the ECDF of configuration 1, Fig. 9 **(b)** of configuration 4, and Fig. 9 **(c)** presents the ECDF of configuration 5. Table V summarizes the results of *Variant 1* of the L/F-CIPS and the lateration baseline considering the aforementioned metrics and configurations. The down arrows in the table indicate that our proposed L/F-CIPS decreases the error with respect to the baseline in the percentage indicated.

B. Results of the Variant 2

Similarly as done in the office scenario and *Variant 1* of the L/F-CIPS, we present the results for the office scenario and *Variant 2* of the L/F-CIPS in Fig. 10 (ECDF) and Table VI (main statistics). In this case, the non-collaborative (stand-alone) method relies on BLE fingerprinting with k-NN.

While the previous results focused on the office scenario with two different approaches for the non-collaborative phase, the next results try to corroborate our finding with a different positioning technology and a different location. We present the results for the lobby scenario and *Variant 2* of the L/F-CIPS in Fig. 11 (ECDF plots) and Table VII (main error statistics). In this case, the non-collaborative (stand-alone) method relies on Wi-Fi fingerprinting with k-NN.

C. Comparison with other collaborative methods

Finally, we compare our proposed L/F-CIPS variants' accuracy to three SOTA CIPSs based on smartphones. Reproducing and replicating the SOTA models available is not straightforward as they may use specific technologies, settings, and/or infrastructure which are not available in our scenarios and collected datasets. Therefore, the comparison is based on published results, which provide a reasonable performance comparison benchmark. Specifically, the comparison involves three aspects: accuracy improvement concerning the baseline system, test conditions, and complexity of the proposed solution.

Taniuchi *et al.* [19] proposed a CIPS based on spring model and homogeneous smartphones using Wi-Fi-fingerprinting and BLE RSS. The system improved the mean accuracy within 2.7%–32.6% in several scenarios. Seco and Jiménez [21] proposed a particle filter approach for CIPS, which relied on smartphones with homogeneous Radio-Frequency Identification (RFID) tags attached to them. The results showed an improvement of 9.09% for the 90$^{\text{th}}$ percentile. Ta *et al.* [22] introduced two CIPS versions based on particle filter and Wi-Fi and BLE RSS values. The implemented versions were tested considering heterogeneous devices in Line-of-sight (LOS) between them in a corridor scenario. The results showed an improvement of the mean accuracy within 5.3%–47.5%.

Our L/F-CIPSs achieved a maximum accuracy improvement of 43.59% and 29.32% regarding the baseline system for the mean and 90$^{\text{th}}$ percentile metrics, respectively. This demonstrates that our system outperforms the CIPS in [19] and [21] in terms of accuracy improvement. However, our L/F-CIPSs has slightly lowest accuracy improvement compared to CIPS presented in [22]. This could be due to our systems being intentionally tested under NLOS conditions between smartphones, which dramatically dropped the system's accuracy.

Regarding complexity, our proposed systems are comparable to CIPS in [22] and [21] based on particle filter. Nevertheless, our system's modularity enables its straightforward implementation and configuration. Moreover, compared with [21], our systems do not rely on additional hardware. Table VIII summarizes the reported results used in the comparison between the SOTA CIPSs and our proposed L/F-CIPS.

TABLE V

MAIN RESULTS METRICS PROVIDED BY THE LATERATION BASELINE AND OUR PROPOSED COLLABORATIVE APPROACH.

Variant 1 – Office	Lateration Error (m)			L/F-CIPS Error (m)			Diff (%)		
Eval. metric	Config. 1	Config. 4	Config. 5	Config. 1	Config. 4	Config. 5	Config. 1	Config. 4	Config. 5
RMSE	4.52	6.98	5.5	2.77	6.1	4.94	↓38.72	↓12.61	↓10.18
Mean	4.29	6.85	4.94	2.42	5.8	4.34	↓43.59	↓15.33	↓12.15
Median	4.11	7.12	5.54	2.09	5.75	4.35	↓49.15	↓19.24	↓21.48
$75th$ percentile	4.76	7.92	6.2	2.93	7.49	5.49	↓38.45	↓5.43	↓11.45
$90th$ percentile	6.72	8.48	8.38	4.75	8.1	8.22	↓29.32	↓4.48	↓1.91

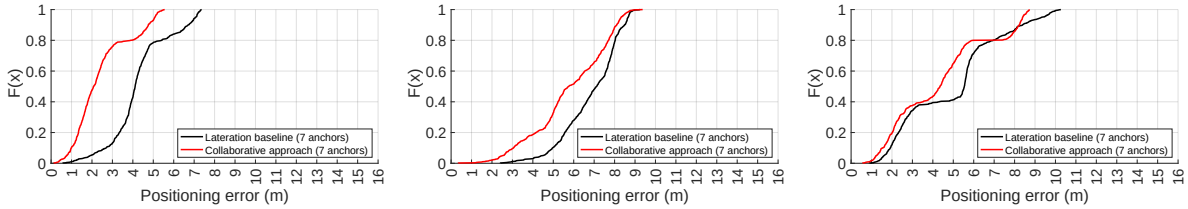

(a) Configuration 1 (b) Configuration 4 (c) Configuration 5

Fig. 9. CDF of the lateration baseline and collaborative approach (7 BLE anchors) of configurations 1, 4, and 5 (office).

TABLE VI

MAIN RESULTS METRICS PROVIDED BY THE BLE FINGERPRINTING BASELINE AND OUR PROPOSED COLLABORATIVE APPROACH.

Variant 2 – Office	BLE Fingerprinting Error (m)			L/F-CIPS Error (m)			Diff (%)		
Eval. metric	Config. 1	Config. 4	Config. 5	Config. 1	Config. 4	Config. 5	Config. 1	Config. 4	Config. 5
RMSE	4.92	4.7	2.54	3.91	4.64	3.72	↓20.53	↓1.28	↑46.46
Mean	4.58	4.25	1.96	3.55	4.12	3.16	↓22.49	↓3.06	↑61.22
Median	4.25	4.16	1.53	3.45	3.86	2.65	↓18.82	↓7.21	↑61.22
$75th$ percentile	5.81	5.31	2.68	4.45	5.67	4.86	↓23.41	↑6.78	↑73.20
$90th$ percentile	7.14	6.97	4.34	5.64	7.06	5.75	↓21.01	↑1.29	↑32.49

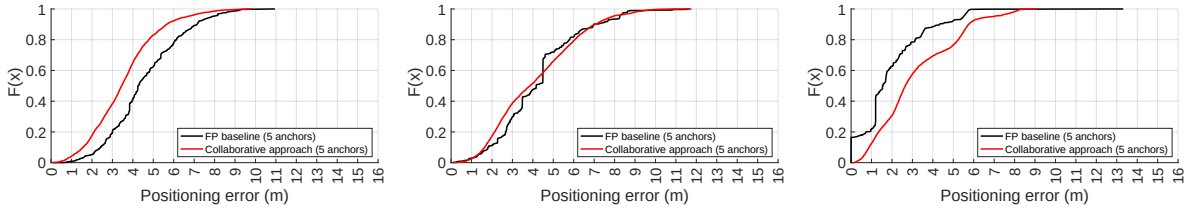

(a) Configuration 1 (b) Configuration 4 (c) Configuration 5

Fig. 10. CDF of the fingerprinting baseline and collaborative approach (5 BLE anchors) of configurations 1, 4, and 5 (office).

TABLE VII

MAIN RESULTS METRICS PROVIDED BY THE WI-FI FINGERPRINTING BASELINE AND OUR PROPOSED COLLABORATIVE APPROACH.

Variant 2 – Lobby	Wi-Fi Fingerprinting Error (m)			L/F-CIPS Error (m)			Diff (%)		
Eval. metric	Config. 1	Config. 4	Config. 5	Config. 1	Config. 4	Config. 5	Config. 1	Config. 4	Config. 5
RMSE	5.83	4.04	5.4	5.37	4.1	6.19	↓7.89	↑1.49	↑14.63
Mean	5.2	3.51	4.86	5	3.68	5.89	↓3.85	↑4.84	↑21.19
Median	4.74	3.18	4.34	5.12	3.59	5.79	↑8.02	↑12.89	↑33.41
$75th$ percentile	7.13	4.62	5.68	6.29	4.92	7.12	↓11.78	↑6.49	↑25.35
$90th$ percentile	9.3	6.25	7.88	7.49	5.88	8.2	↓19.49	↓5.92	↑4.06

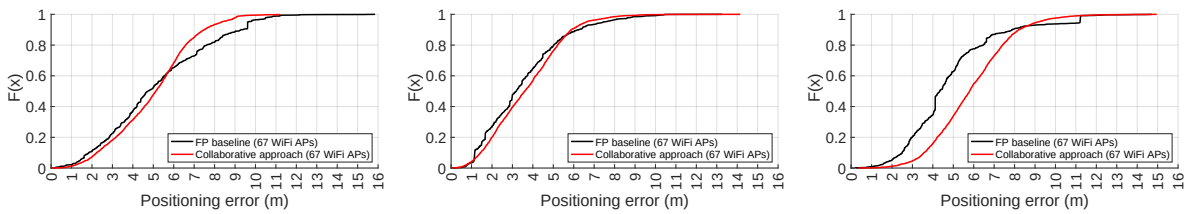

(a) Configuration 1 (b) Configuration 4 (c) Configuration 5

Fig. 11. CDF of the fingerprinting baseline and collaborative approach (67 Wi-Fi APs) of configurations 1, 4, and 5 (lobby).

Overall, our proposed systems achieve comparable or better accuracy than the existing systems, while using heterogeneous devices and NLOS conditions in the test scenarios. These improvements are obvious when using collaborative approaches compared to the baseline approaches; it is to be noted that the baseline error performance differs from scenario to scenario because different measurement datasets were used.

TABLE VIII
COMPARISON OF SOTA CIPSS VS PROPOSED L/F-CIPS

Ref.	NLOS Conditions	Device Diversity	Evaluation Metrics	Baseline error (m)	CIPS error (m)	Diff (%)
[19]	Y	N	Mean	2.08	2.02	↓2.7 (Min)
				1.45	0.98	↓32.6 (Max)
[21]	Y	N	90th Per.	4.4	4	↓9.09
[22]	N	Y	Mean	3.8	3.6	↓5.3 (Min)
				4	2.1	↓47.5 (Max)
Ours Var.1	Y	Y	Mean	4.29	2.42	↓43.59 (Max)
			90th Per.	6.72	4.75	↓29.32 (Max)
Ours Var.2	Y	Y	Mean	4.58	3.55	↓22.49 (Max)
			90th Per.	7.14	5.64	↓21.01 (Max)

D. Discussion

The *Variant 1* of the L/F-CIPS, which considers BLE technology, was tested in an office scenario and compared to lateration. We considered three configurations, covering short, medium, and large distances among devices. As shown in Table V, our proposed collaborative approach performs better than lateration in all the evaluation metrics for all the configurations evaluated. Specifically, in short distances (configuration 1), medium distances (configuration 4), and large distances (configuration 5) the maximum difference are 49.15 %, 19.24 %, and 21.48 % for the median metric, respectively.

Moreover, considering the relative difference of the RMSE, mean and 75th percentile, we can observe that our proposed collaborative approach significantly outperforms lateration in short distances, moderately in medium distances and slightly in large distances. According to the ECDF plots (see Figure 9), our collaborative approach greatly outperforms lateration baseline in all the cases in short distances. In medium distances, the proposed collaborative method is better than lateration, but differences are short after the 70th percentile. For large distances, the proposed method is better until the 80th percentile. Additionally, in Figure 9 (a) and (c), there are small flat sections at 0.8 and (0.4 and 0.8) for configuration 1 and 5, respectively, in both the lateration and collaborative approaches. This indicates that there are no cases with positioning errors falling within those specific error ranges. For example, around 3 m to around 4 m in Figure 9 (a) errors fall in an area following (almost) a normal distribution, but in some cases, such as in Figure 9 (a), there is a reference point with extremely large positioning error. As a result, the error in 4 reference points is around 0 to 3 meters, while in the most distant reference point, the error is above 4 m. A similar situation occurs in Figure 9 (c), where the error is low in 2 reference points, moderate in 2 other reference points and large in 1 reference point.

It is worth mentioning that lateration positioning accuracy was significantly worse than RSS in the literature [16], [23]. Our real-world test scenario conditions include hardware heterogeneity (smartphones), strong NLOS and poor/inappropriate distribution of the BLE anchors. Nevertheless, the error values obtained are consistent with challenging scenarios in the literature [24].

The *Variant 2* of the L/F-CIPS was first evaluated on the same office scenario. The results reported in Table VI and Fig. 10 show that our collaborative approach greatly outperforms the stand-alone fingerprinting in all evaluation metrics when the mobile devices are very near to each other (configuration 1). When the distance among devices is short, the signal propagation presents less attenuation and reduced multipath. When the distance among devices is medium, our proposed CIPS is better than fingerprinting below the 60th percentile and above the 90th percentile (large errors area). In this case, the physical obstruction and multipath propagation due to surrounding objects are frequent. However, when the distance among devices is large, the performance of our proposed L/F-CIPS is worse than fingerprinting. Fig. 10 (b) and (c) present vertical flat sections similar to those in Figure 9 (a) and (c) due to the distribution of reference points in the scenario.

The *Variant 2* was also evaluated in the lobby scenario. The results reported in Table VII and Fig. 11 show that our collaborative approach outperforms the stand-alone approach in the short distance case. Unlike the office scenario, its performance is more moderate, reducing the error in four of five evaluation metrics. In the medium distance, we observe that until the 80th percentile, the stand-alone approach slightly outperforms the proposed collaborative method, but in the remaining cases, the collaborative approach outperforms fingerprinting. In the large distance case, we just notice that our approach moderately improves fingerprinting after the 90th percentile. It seems that Wi-Fi fingerprinting is less reliable for stand-alone positioning in collaborative frameworks. However, the collaborative approach benefits from the increasing number of devices in real-life indoor scenarios, resulting in improved accuracy due to higher device density and closer proximity. Additionally, more devices participating in collaboration enhance data availability, leading to better accuracy and coverage.

VI. CONCLUSION

In this paper, we have proposed L/F-CIPS, a collaborative approach to enhance positioning accuracy for pedestrians using smart devices. It uses a novel way to estimate relative distances using a Multilayer Perceptron (MLP) Artificial Neural Networks (ANNs) model instead of the traditional Logarithm Distance Path Loss (LDPL) model. The proposed estimator not only considers the Received Signal Strength (RSS) value but also the calibration of the receiver and the stand-alone positions of the two involved devices.

We have evaluated the proposed L/F-CIPS using two positioning technologies (Wi-Fi and BLE), two methods (lateration and fingerprinting) and two real-world scenarios (office and lobby) in two different countries.

The results have demonstrated the usefulness of our proposed L/F-CIPS architecture to develop new CIPS considering diverse technologies and methods to improve the positioning accuracy of traditional lateration and fingerprinting. Specifically, *Variant 1*, based on RSS lateration, improves the positioning performance of traditional lateration in all the tested configurations (i.e., where the devices have short, medium, and large distances among them). In contrast, *Variant 2*, based on RSS fingerprinting, demonstrated that L/F-CIPS enhances the positioning accuracy of traditional IPSs based on fingerprinting under specific conditions. In this last case, the distance among devices should preferably be short to get a significant gain.

Considering the state of the art CIPSs tested under NLOS conditions, our *Variant 1* outperforms them by 10.99% and 20.23% with respect to the maximum difference of the mean and 90th percentile, respectively. Furthermore, testing our proposed L/F-CIPSs showed that the use of BLE provides better positioning accuracy than Wi-Fi technology and that the large inter-device distance distributions decrease the accuracy of our L/F-CIPSs. Nevertheless, for moderate or high-density of smartphones – and thus short and medium inter-device distances – as present in real indoor scenarios, our proposal provides an improvement compared to IPSs. In general, the integration of the MLP ANNs model in CIPSs allows us to use our approach under different scenarios and for different technologies, showing its generality, feasibility, and usefulness.

Future work will include improving large inter-device distance estimation by exploring advanced machine-learning methods which use as input screenshot images based on the scenario area, the devices' estimated position, and RSS. In addition, we will explore an iterative version of our approach, where the position estimates will be iteratively refined while keeping a low computational cost.

REFERENCES

[1] *Indoor Location Based Services Market Research Report by Technology, Device, Industry, Application, and Region - Global Forecast to 2026 - Cumulative Impact of COVID-19*, https://www.researchandmarkets.com/reports/4896758/, 2021.

[2] R. Liu, Z. Yin, *et al.*, "Wibeacon: Expanding ble location-based services via wifi," in *Proceedings of the 27th Annual International Conference on Mobile Computing and Networking*, 2021, pp. 83–96.

[3] P. Uphaus, B. Beringer, *et al.*, "Location-based services–the market: Success factors and emerging trends from an exploratory approach," *Journal of Location Based Services*, vol. 15, no. 1, pp. 1–26, 2021.

[4] P. Spachos and K. N. Plataniotis, "Ble beacons for indoor positioning at an interactive iot-based smart museum," *IEEE Systems Journal*, vol. 14, no. 3, pp. 3483–3493, 2020.

[5] S. Sadowski and P. Spachos, "Optimization of ble beacon density for rssi-based indoor localization," in *2019 IEEE International Conference on Communications Workshops (ICC Workshops)*, IEEE, 2019.

[6] G. M. Mendoza-Silva, M. Matey-Sanz, *et al.*, "Ble rss measurements dataset for research on accurate indoor positioning," *Data*, vol. 4, no. 1, p. 12, 2019.

[7] K. E. Jeon, J. She, *et al.*, "Ble beacons for internet of things applications: Survey, challenges, and opportunities," *IEEE Internet of Things Journal*, vol. 5, no. 2, pp. 811–828, 2018.

[8] T.-Y. Tsai, C.-C. Hsu, *et al.*, "Mobile localization-based service based on rssi fingerprinting method by ble technology," in *IEEE International Conference on Consumer Electronics-Berlin*, 2018.

[9] T.-M. T. Dinh, N.-S. Duong, *et al.*, "Smartphone-based indoor positioning using ble ibeacon and reliable lightweight fingerprint map," *IEEE Sensors Journal*, vol. 20, no. 17, pp. 10 283–10 294, 2020.

[10] P. Pascacio, S. Casteleyn, *et al.*, "Smartphone distance estimation based on rssi-fuzzy classification approach," in *2021 International Conference on Localization and GNSS (ICL-GNSS)*, IEEE, 2021.

[11] P. Pascacio, J. Torres–Sospedra, *et al.*, "A collaborative approach using neural networks for ble-rss lateration-based indoor positioning," in *2022 International Joint Conference on Neural Networks (IJCNN)*, IEEE, 2022, pp. 01–09.

[12] P. Pascacio, S. Casteleyn, *et al.*, "Collaborative indoor positioning systems: A systematic review," *Sensors*, vol. 21, no. 3, p. 1002, 2021.

[13] A. Ozer and E. John, "Improving the accuracy of bluetooth low energy indoor positioning system using kalman filtering," in *2016 International Conference on Computational Science and Computational Intelligence (CSCI)*, IEEE, 2016, pp. 180–185.

[14] F. Zafari, I. Papapanagiotou, *et al.*, "A novel bayesian filtering based algorithm for rssi-based indoor localization," in *2018 IEEE International Conference on Communications (ICC)*, IEEE, 2018.

[15] A. Booranawong, K. Sengchuai, *et al.*, "Rssi-based indoor localization using multi-lateration with zone selection and virtual position-based compensation methods," *IEEE Access*, vol. 9, pp. 46 223–46 239, 2021.

[16] P. Pascacio, J. Torres-Sospedra, *et al.*, "A lateration method based on effective combinatorial beacon selection for bluetooth low energy indoor positioning," in *2021 17th International Conference on Wireless and Mobile Computing, Networking and Communications (WiMob)*, IEEE, 2021, pp. 397–402.

[17] R. Santos, M. Barandas, *et al.*, "Fingerprints and floor plans construction for indoor localisation based on crowdsourcing," *Sensors*, vol. 19, no. 4, p. 919, 2019.

[18] W. Li, D. Wei, *et al.*, "Geomagnetism-aided indoor wi-fi radio-map construction via smartphone crowdsourcing," *Sensors*, vol. 18, no. 5, p. 1462, 2018.

[19] D. Taniuchi, X. Liu, *et al.*, "Spring model based collaborative indoor position estimation with neighbor mobile devices," *IEEE Journal of Selected Topics in Signal Processing*, vol. 9, no. 2, pp. 268–277, 2014.

[20] T. Dag and T. Arsan, "Received signal strength based least squares lateration algorithm for indoor localization," *Computers & Electrical Engineering*, vol. 66, pp. 114–126, 2018.

[21] F. Seco and A. R. Jiménez, "Smartphone-based cooperative indoor localization with rfid technology," *Sensors*, vol. 18, no. 1, p. 266, 2018.

[22] V.-C. Ta, T.-K. Dao, *et al.*, "Collaborative smartphone-based user positioning in a multiple-user context using wireless technologies," *Sensors*, vol. 20, no. 2, p. 405, 2020.

[23] F. Subhan, A. Khan, *et al.*, "Experimental analysis of received signals strength in bluetooth low energy (ble) and its effect on distance and position estimation," *Transactions on Emerging Telecommunications Technologies*, e3793, 2019.

[24] K. Cengiz, "Comprehensive analysis on least-squares lateration for indoor positioning systems," *IEEE Internet of Things Journal*, vol. 8, no. 4, pp. 2842–2856, 2020.

Pavel Pascacio is currently an Early Stage Researcher of the A-WEAR project and is pursuing a European Joint Doctorate in Universitat Jaume I (Spain) and Tampere University (Finland). He received his Master's Degree in Automation and Control Engineering from Politecnico di Milano, Italy, in 2019.

Joaquín Torres-Sospedra is Senior Researcher at the University of Minho (Guimarães, Portugal), where he works on Indoor Positioning and Machine Learning for Industrial applications. He has authored more than 170 articles in journals and conferences; and supervised 16 Master and 6 PhD Students. He is the chair of the IPIN International Standards Committee and IPIN Smartphone-based off-site Competition.

Sven Casteleyn received his master's degree (1999) in informatics and Ph.D. degree (2005) in science from Vrije Universiteit Brussel, Belgium. He is currently an Associate Professor at the Geospatial Technologies Research Group, part of the Institute of New Imaging Technologies, Universitat Jaume I, Castellón de la Plana, Spain. His research focuses on Web and mobile systems, geographical information science and technology and their application fields, and (mental) health informatics.

Elena Simona Lohan (S'00, M'06, SM'13) received an MSc degree in Electrical Engineering from Polytechnics University of Bucharest, Romania, in 1997, a DEA degree in Econometrics, at Ecole Polytechnique, Paris, France, in 1998, and a PhD degree in Telecommunications from Tampere University of Technology, Finland, in 2003. Dr. Lohan is now a Full Professor at the Electrical Engineering unit at Tampere University. She is a co-editor of two books on positioning and has co-authored more than 185 international peer-reviewed publications and 6 patents and inventions. She is also the coordinator of A-WEAR MSCA-EJD Doctorate network. Her current research interests include wireless location techniques, GNSS for aviation, wearables, and privacy-aware positioning solutions.

Jari Nurmi, D.Sc.(Tech) 1994, is Professor at Tampere University (formerly Tampere University of Technology), Finland since 1999. He works on embedded computing, wireless localization, and software-defined radio/networks. He held various positions at TUT 1987-1994 and was the Vice President of SME VLSI Solution Oy 1995-1998. He has supervised 30 PhD and over 150 MSc theses, and been opponent/reviewer of about 50 PhD theses worldwide. He is senior member of IEEE, member of the technical committee on VLSI Systems and Applications at IEEE CASS, and in steering committees of four international conferences (chairman in two). He has edited five Springer books, and published over 400 international publications. Dr. Nurmi is also associate editor of three international journals, and the director of national DELTA doctoral training network of over 200 PhD students.